Doubly Tapered Electromagnetic Periodic Structure (DT-EPS) for Planar and Cylindrical Coplanar Waveguide (CPW) Applications

Yu Zhen WANG, Man Long HER, Yi Chyun CHIOU, and Ying De WU
Wireless Communications Lab, Department of Communications Engineering, Feng-Chia University
100 Wenhua Rd., Seatwan, Taichung 407, Taiwan.
p9126221@knight.fcu.edu.tw

1. Introduction

The electromagnetic periodic structure (EPS) was first introduced to control lightwave propagation in the optical frequency bands. Recently, the EPS has been utilized in several microwave and millimeter wave circuits such as resonators, antennas, and other applications to provide stopband and slow-wave characteristics in one or more frequency ranges [1]-[5]. For applications in bandstop filters, the EPS is usually formed by etching periodic cells of shapes such as rectangles and circles in the ground plane. With properly designed EPS, the propagation of electromagnetic wave is forbidden in some specified frequency bands. In the previous work, it was found the conventional tapered EPS not only could increase the bandwidth of the stopband but reduce the sidelobe of the passband as well [6]. However, it was also shown that the stopband rejection was degraded. In this paper, we proposed the doubly tapered EPS (DT-EPS) which implements EPS cells both in signal strip and ground plane to improve the performance of bandstop filters in coplanar waveguide (CPW) and cylindrical coplanar waveguide (CCPW) technologies [7]-[9].

2. EPS Design and Analysis

The CPW bandstop filter with conventional tapered EPS and in the planar substrate is shown in Fig. 1. It is constructed by etching nine square cells with periodicity along the axial direction in the ground plane. To achieve the bandstop characteristics, the period of the EPS, d, should satisfy $\beta = \pi / d$, where β is wave propagation constant of the guided wave. For $\beta = 2\pi / \lambda_g$, the period of the EPS is equal to $\lambda_g / 2$. Besides, the tapered technique was designed following a Hamming window distribution, for which the length of each of the EPS cell, $a(z)$, must satisfy the following equation [10]:

$$a(z) = a_0 \times (0.54 - 0.46\cos(2\pi z / L)) \quad (1)$$

where z is the distance measured from the edge of the circuit board, a_0 is the peak amplitude of the tapered cell and L is the total length of the filter.

Fig. 2(a) is an enlarged version of the peak amplitude of the proposed DT-EPS unit cell. In order to observe the effect of the alignment offset with the parameter of x, we simulate the DT-EPS and tune its alignment offset to compare with uniform case by high frequency simulator Ansoft HFSS. The alignment offset, x, can be expressed as the following equation:

$$x = s/4 - a_0/2 - b_0 \quad (2)$$

where b_0 is the distance between the edge of the EPS cell and slot.

The bandstop filters in this paper were implemented on Roger/RO3003 substrate with relative dielectric constant $\varepsilon_r = 3$ and thickness h = 0.75 mm. The center stopband frequency was designed to be near 10 GHz. With above-mentioned material parameters, the signal strip (s) and the slot width (w) were calculated to be 4.6 mm and 0.25 mm, respectively, corresponding to a strip characteristic impedance of 50 ohms. Fig. 2(b) depicts the simulated results of uniform EPS and the DT-EPS with x = 0 mm and 0.15 mm alignment offset. In Fig. 2(b), the stopband rejection of DT-EPS with x = 0.15 mm alignment offset at 10 GHz center frequency is much deeper than uniform case. We can utilize circuit and surface current concepts to interpret this phenomenon. The improved performance in doubly EPS can be explained as that the additional transverse slot at signal strip introduces a series LC tank in the forward current path. Thus, it equivalently increases the order of the bandstop filter.

ISBN: 4-88552-206-4 C3055©IEICE

Moreover, the doubly EPS with 0.15 alignment offset increases longer path of current of the propagation mode than another 0 mm alignment offset. This improves the effect of slow-wave characteristic of the filter, and hence shifts down its resonance frequency. Fig. 3 depicts the proposed DT-EPS in CCPW structure, for a realizable radius r of 17 mm is corresponding to curvelinear coefficient $R = r/(r+h)$ of 0.958 and the rest of the geometrical parameters are the same of those of the CPW structure.

3. Measured Results and Discussion

The measured CPW bandstop filter is shown in Fig. 4. In Fig. 4(a), the insertion loss of the uniform and conventional tapered EPS with different peak amplitude is measured. The first peak level of the lower passband ripples is improved from –4 dB of the lower uniform EPS to –0.5 dB of the conventional tapered with a_0 = 2 mm. However, the stopband rejection of the conventional tapered EPS is degraded. In order to overcome the degradation of stopband rejection on conventional tapered EPS, the method of increasing peak amplitude is recommended. Although the stopband rejection is improved while a_0 = 3 mm, the upper passband loss is getting larger at the same time. Therefore, the DT-EPS technique is proposed to improve the phenomenon of upper passband loss. Fig. 4(b) depicts the measured the insertion loss of the uniform EPS, conventional tapered EPS and DT-EPS with a_0 = 2 mm. In Fig. 4(b), it is shown that the proposed DT-EPS improves the –20 dB bandwidth from 28% of the uniform EPS case to 38%. Moreover, the stopband rejection is improved from –16 dB of conventional tapered one to –34 dB, while the upper passband loss can still be maintained as lower level than uniform EPS. Fig. 4(c) illustrates the measured return loss of all EPS. In Fig. 4(c), it is found that both tapered EPS have comparable lower sidelobe levels.

Fig. 5 depicts measured results of uniform EPS, conventional tapered EPS, and DT-EPS in CCPW technology. Fig. 5(a) presents the measured insertion loss of uniform EPS and conventional tapered EPS in CCPW technology with a_0 = 2 mm and 3 mm. The closet results between Fig. 4(a) and Fig. 5(a) are obtained. Fig. 5(b) illustrates the measured insertion loss of uniform EPS, conventional EPS and DT-EPS in CCPW structure. In Fig. 5(b), the DT-EPS technique improves the –20 dB bandwidth from 20% of the uniform EPS case to 32%. The stopband rejection is improved from –14 dB of conventional tapered EPS to –35 dB without any degradation of the upper passband. Fig. 5(c) shows return loss of both tapered EPS is better than the uniform EPS case. The achievements of using the DT-EPS technique in planar structure are also applicable in CCPW structure.

4. Conclusion

In this paper, the CPW bandstop filters fabricated on both planar and cylindrical substrates with DT-EPS were implemented and analyzed. Besides, the relationships among all bandstop filters in stopband rejection, stopband bandwidth, upper and lower passband ripples have been investigated. Measured results show that the proposed DT-EPS designed with Hamming windows distribution has demonstrated its ability to reduce lower, upper passband ripples and improve stopband bandwidth compared with uniform case. The DT-EPS technique can also be applied in several microwave and millimeter wave circuits such as antennas, power amplifiers and other applications.

5. Acknowledgement

The authors would like to thank the assistance and support of Professor Chin-Her Lee and Mr. Chih-Ming Chang who are with Department of Electronic Engineering at National Changhua university of Education in Taiwan and Benq Corp. in Taiwan, respectively.

6. References

[1] T. Y. Yun, and K. Chang, “Uniplanar one-dimensional phtonic-bandgap structures and resonators,” *IEEE Trans. Microwave Theory & Tech.*, vol. 49, no. 3, pp. 547-533, March 2001.
[2] F. Y. Yang, K. P. Ma, Y. Qian, and T. Itoh, “A uniplanar compact photonic-bandgap (UC-PBG) structure and its applications for microwave circuits,” *IEEE Trans. Microwave Theory & Tech.*, vol. 47, no. 8, pp. 1509-1514, August 1999.
[3] D. Sievenpiper, L. Zhang, R. F. J. Broas, G. N. Alexopolous, and E. Yablonovitch, “High-impedance electromagnetic surfaces with a forbidden frequency band,” *IEEE Trans. Microwave Theory & Tech.*, vol. 47, no. 11, pp. 2059-2074, November 1999.
[4] V. Radisic, Y. Qian, and T. Itoh, “Broad-band power amplifier using dielectric photonic bandgap structure,” *IEEE Guided Wave Letters*, vol. 8, no. 1, pp. 13-14, January 1998.

[5] M. Harris, “Summary on preferred terminology to replace ‘photonic bandgap’ in describing microwave and millimeter wave periodic structures,” *IEEE Microwave Magazine*, vol. 3, pp. 75, September 2002.
[6] T. Lopetegi, F. Falcone, B. Matinez, R. Gonzalo, and M. Sorolla, “Improved 2-D photonic bandgap structure in microstrip technology,” *Microwave and Optical Technology Letters*, vol. 22, no. 3, pp. 207-211, August 1999.
[7] C. M. Chang, “Design and analysis of CPW filters with slow-wave and PBG structures,” *Thesis, Feng-Chia University*, Taiwan, July 2002.
[8] M. L. Her, C. M. Chang, Y. Z. Wang, F. H. Kung, and Y. C. Chiou, “Improved coplanar waveguide (CPW) banstop filter with photonic bandgap (PBG) structure,” *Microwave and Optical Technology Letters*, vol. 38, no. 4, pp. 274-277, August 2003.
[9] M. L. Her, Y. Z. Wang, Y. C. Chiou, and F. H. Kung, “Improved doubly tapered electromagnetic periodic structure (EPS) for bandstop filter applications,” *IEICE Trans. Electron.*, vol. E86-C, no. 10, pp. 2151-2153, October 2003.
[10] C. K. Chong, D. B. McDermott, M. M. Razeghi, N. C. Luhmann Jr., J. Pretterebner, D. Wagner, M. Thumm, M. Caplan, and B. Kulke, “Bragg reflectors,” *IEEE Trans. Plasma Sci.*, vol. 20, no. 3, pp. 393-402, June 1992.

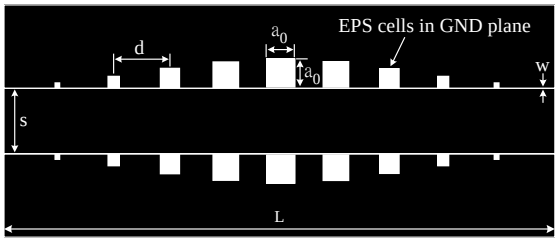

Fig. 1 Schematic Diagram of the conventional tapered EPS in CPW structure.

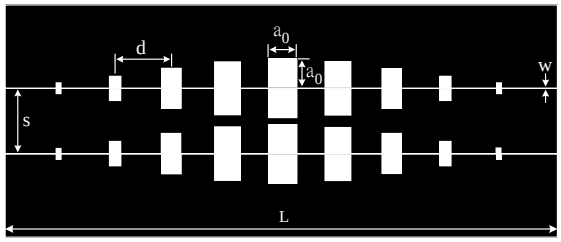

(a)

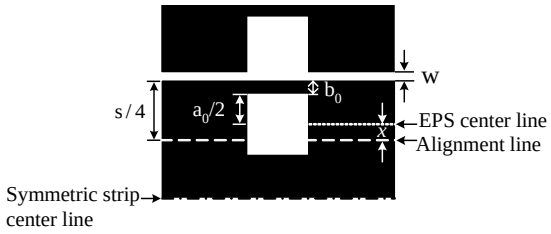

(a)

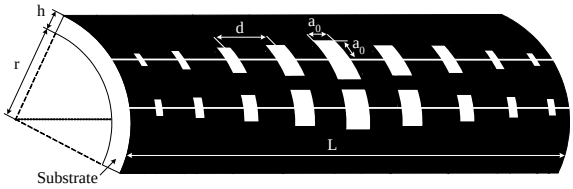

(b)

Fig. 3(a) Schematic diagram of the DT-EPS in CPW structure. (b) Schematic diagram of the DT-EPS in CCPW structure.

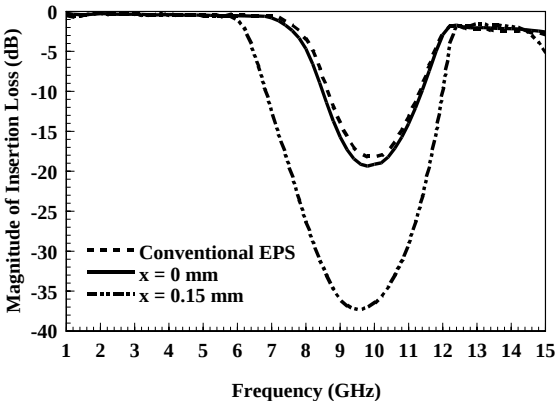

(b)

Fig. 2(a) An enlarged version of the peak amplitude of the unit cell of the DT-EPS in CPW structure, where a_0 = 2 mm. (b) Simulated results of the insertion loss for comparison among conventional tapered EPS and DT-EPS with x = 0 mm and x = 0.15 mm alignment offset.

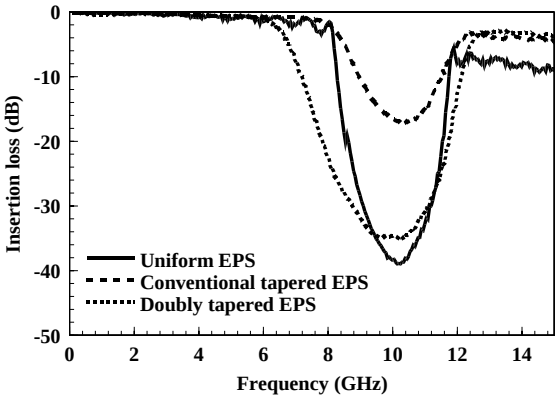

(a)

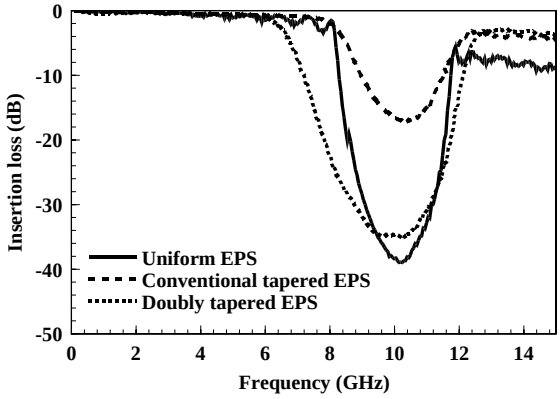

(b)

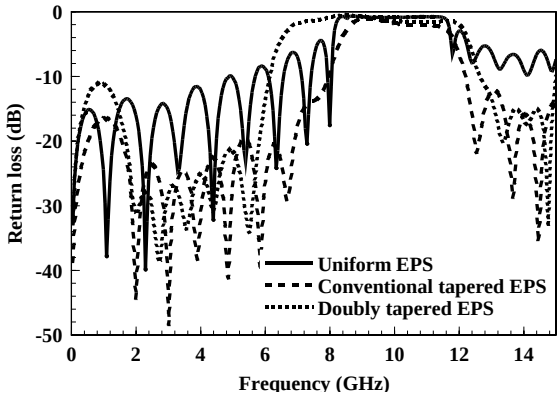

(c)

Fig. 4(a) Measured insertion loss of uniform EPS and conventional tapered EPS with a_0 = 2 mm and 3 mm; (b) measured insertion loss of uniform EPS, conventional tapered EPS and DT-EPS with a_0 = 2 mm; (c) measured return loss of uniform EPS, conventional tapered EPS and DT-EPS with a_0 = 2 mm.

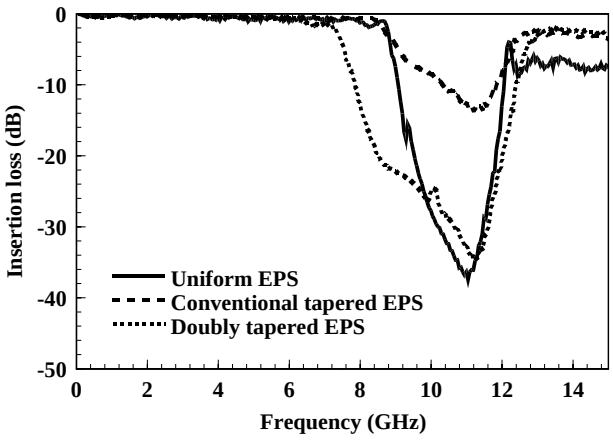

(a)

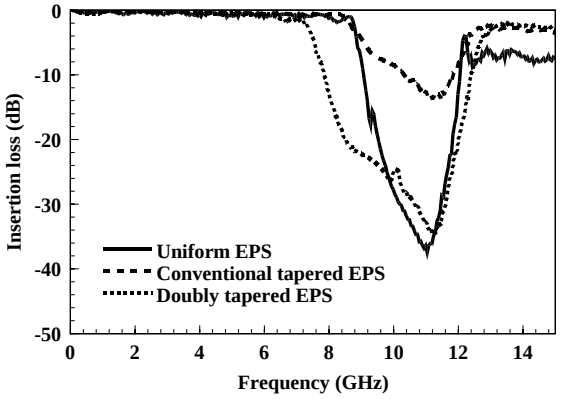

(b)

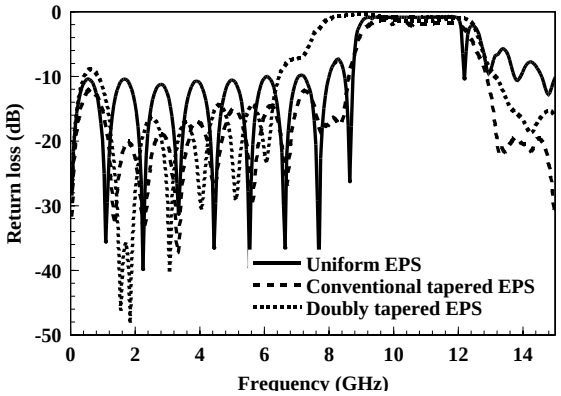

(c)

Fig. 5(a) Measured insertion loss of uniform EPS and conventional tapered EPS with a_0 = 2 mm and 3 mm in CCPW technology; (b) measured insertion loss of uniform EPS, conventional tapered EPS and DT-EPS with a_0 = 2 mm in CCPW technology; (c) measured return loss of uniform EPS, conventional tapered EPS and DT-EPS with a_0 = 2 mm in CCPW technology